Improved Indirect Limits on Muon Electric Dipole Moment

Yohei Ema,[1,*] Ting Gao,[2,†] and Maxim Pospelov[2,3,‡]

[1]*Deutsches Elektronen-Synchrotron DESY, Notkestraße 85, 22607 Hamburg, Germany*

[2]*School of Physics and Astronomy, University of Minnesota, Minneapolis, Minnesota 55455, USA*

[3]*William I. Fine Theoretical Physics Institute, School of Physics and Astronomy, University of Minnesota, Minneapolis, Minnesota 55455, USA*

(Received 5 October 2021; revised 27 January 2022; accepted 7 March 2022; published 1 April 2022)

Given current discrepancy in muon $g-2$ and future dedicated efforts to measure muon electric dipole moment (EDM) d_μ, we assess the indirect constraints imposed on d_μ by the EDM measurements performed with heavy atoms and molecules. We notice that the dominant muon EDM effect arises via the muon-loop induced "light-by-light" CP-odd amplitude $\propto \mathbf{BE}^3$, and in the vicinity of a large nucleus the corresponding parameter of expansion can be significant, $eE_{\rm nucl}/m_\mu^2 \sim 0.04$. We compute the d_μ-induced Schiff moment of the ^{199}Hg nucleus, and the linear combination of d_e and semileptonic C_S operator (dominant in this case) that determine the CP-odd effects in the ThO molecule. The results, $d_\mu(^{199}\mathrm{Hg}) < 6\times10^{-20}$ e cm and $d_\mu(\mathrm{ThO}) < 2\times10^{-20}$ e cm, constitute approximately threefold and ninefold improvements over the limits on d_μ extracted from the Brookhaven National Laboratory muon beam experiment.

DOI: 10.1103/PhysRevLett.128.131803

Introduction.—The searches for electric dipole moment (EDMs) of elementary particles have progressed a long way since the first indirect limit on neutron EDM found by Purcell and Ramsey seventy years ago [1]. Current precision improved by nearly 10 orders of magnitude since [1] and nil results of the most precise measurements [2–5] have served a death warrant to many models that seek to break CP symmetry at the weak scale in a substantial way (see, e.g., [6–9]).

EDMs of neutron and heavy atoms can also serve to constrain EDMs of heavier particles that do not appear inside these light objects "on-shell" [10]. While for the EDMs (and color EDMs) of heavy quarks the gluon mediation (and for heaviest objects such as t quark, Higgs mediation) diagrams play a crucial role [11,12], the EDMs of muons and τ leptons require three-loop $\alpha_{\rm EM}^3$ suppressed amplitudes to generate the electron EDM d_e via radiative corrections [13]. In this Letter, we reevaluate the muon EDM (d_μ) induced CP-odd observables and find the enhanced sensitivity to d_μ in experiments that measure EDMs of heavy atoms and molecules.

The latest interest to muons is fueled by the ongoing discrepancy between theoretical predictions and experimental measurement of the muon anomalous magnetic moment [14–20]. It brings into focus a question of other observables that involve muons, and one such important quantity is the muon EDM, d_μ (see, e.g., [21] on extended discussion on this point). At the moment, the auxiliary EDM measurement at the Brookhaven $g-2$ experiment sets the tightest bound on muon EDM [22],

$$|d_\mu| < 1.8\times10^{-19}\ e\,\mathrm{cm}, \tag{1}$$

but there are proposals on significantly improving this bound with dedicated muon beam experiments [23–26]. Given these upcoming efforts it is important to reevaluate *indirect* bounds on muon EDM, especially given significant progress in precision of atomic and molecular EDM experiments in recent years.

In this Letter, we evaluate indirect limits on d_μ finding superior bounds to (1) from Hg and ThO EDM experiments [2,4]. Our results draw heavily on the fact that the closed muon loop with d_μ insertion is placed in a very strong electric field of a large nucleus (e.g., Hg or Th). The resulting interaction, encapsulated by the $\mathbf{E}^3\mathbf{B}$ effective operator, is capable of generating Schiff moment [27], CP-odd electron-nucleus interaction [6], and magnetic quadrupole moment. Below, we elaborate on details of our findings (see also [28]).

Muon EDM and E^3B interaction.—The input into our calculations is the muon EDM operator,

$$\mathcal{L}_{CP\text{-odd}} = -\frac{i}{2}F^{\alpha\beta}\times\bar{\mu}\sigma_{\alpha\beta}\gamma_5\mu\times d_\mu, \tag{2}$$

and for the purpose of this Letter we assume that the Wilson coefficient d_μ is the only source of CP violation.

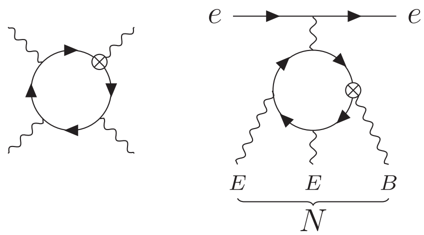

FIG. 1. A representative light-by-light scattering diagram with d_μ insertion (indicated by the crossed dot) giving rise to E^3B interaction. When E^2B is sourced by the nucleus, as shown on the right, d_N and S_N are generated.

At one loop order, muons induce CP-odd nonlinear electromagnetic interactions, much the same as the well-studied "light-by-light" diagrams in the CP-even channel. In Fig. 1 we show an example of such a diagram. We notice that photon momenta entering the muon loop are small compared to the muon mass m_μ. Indeed, in a large nucleus, $q_\gamma^{\max} \sim R_N^{-1} \sim 30$ MeV, one can truncate the series to the lowest dimension operator, and assume electric $\mathbf{E}$ and magnetic $\mathbf{B}$ fields to be uniform. Working in the lowest order in d_μ, we directly compute the corresponding electromagnetic operators, similar to the dimension eight term in the Euler-Heisenberg Lagrangian:

$$\mathcal{L} = -e^4(\tilde{F}_{\alpha\beta}F^{\alpha\beta})(F_{\gamma\delta}F^{\gamma\delta}) \times \frac{d_\mu/e}{96\pi^2 m_\mu^3}$$
$$= -\frac{d_\mu/e}{12\pi^2 m_\mu^3} e^4(\mathbf{E}\cdot\mathbf{B})(\mathbf{E}\cdot\mathbf{E} - \mathbf{B}\cdot\mathbf{B}), \quad (3)$$

where $\tilde{F}_{\alpha\beta} = \frac{1}{2}\epsilon_{\alpha\beta\mu\nu}F^{\mu\nu}$, and we define the gauge coupling e to be positive. One can notice interesting differences with the CP-even case: the dimension four $(\tilde{F}_{\alpha\beta}F^{\alpha\beta})$ operator can be dropped, and there is only one dimension eight operator $(FF)(F\tilde{F})$, while the CP-even case has two, $(FF)(FF)$ and $(F\tilde{F})(F\tilde{F})$. The effective CP-odd photon interactions were discussed recently in [31]. In principle, all terms in the expansion can be computed analytically. Neglecting the $O(B^3)$ interaction that is subdominant due to no Z enhancement leaves only the E^3B effective operator that we write in a more generic form that can be applied to other sources of CP violation as well:

$$H_{\text{eff}} = C_{E^3B} \times \int d^3x e^4(\mathbf{E}\cdot\mathbf{E})(\mathbf{E}\cdot\mathbf{B}), \quad (4)$$

with $C_{E^3B} = (12\pi^2 m_\mu^3)^{-1} d_\mu/e$ in our model (2).

It is important to note that the E^3B effective interaction does not always capture all relevant physics. For example, the muon-loop-mediated electron EDM that arises at three loop order involves computation with loop momenta that can be comparable or even larger than m_μ. In that case, the entire CP-odd four-photon amplitude is needed [13]. In what follows we evaluate the physical consequences of the E^3B interaction.

Muon EDM and nuclear CP-odd observables.—Nuclear spin dependent EDMs (sometimes called diamagnetic EDMs) provide stringent tests of CP violation via probing nuclear T, P-odd moments. At this step we address the mechanisms that convert CP-even static nuclear moments to the CP-odd ones,

$$\mu_N, Q_N \xrightarrow{E^3B} d_N, S_N, M_N, \quad (5)$$

where subscript N stands for "nuclear," and μ, Q, d, S, M are magnetic, electric quadrupole, electric dipole, Schiff, and magnetic quadrupole moments. (Inside a neutral atom, d_N is not observable by itself, but in the linear combination that parametrizes the difference between EDM and charge distribution, the Schiff moment [27]).

Consider a spin-$\frac{1}{2}$ nucleus, as in the most sensitive diamagnetic EDM experiment with ^{199}Hg [2]. Then M_N is absent by definition, but d_N and S_N can be induced as shown in Fig. 1. To calculate them we notice that the magnetic field of the $I = 1/2$ nucleus can be presented in the following form:

$$eB_i(\mathbf{r}) = b_1(r)n_{Ii} + b_2(r)(3n_in_j - \delta_{ij})n_{Ij}, \quad (6)$$

where we introduced the unit vector in the direction of the nuclear spin, $\mathbf{n}_I = \mathbf{I}/I$, $\mathbf{n} = \mathbf{r}/r$ and some scalar invariant functions $b_{1(2)}(r)$. Notice that in the limit of a very small nuclear radius, $R_N \to 0$, the corresponding asymptotics of these functions are

$$b_1(r) \to \frac{2e\mu_N}{3}\delta(\mathbf{r}); \qquad b_2(r) \to \frac{e\mu_N}{4\pi r^3}, \quad (7)$$

where μ_N is the nuclear magnetic dipole moment value. The nuclear electric field, to good accuracy, can be described by the radial ansatz,

$$e\mathbf{E} = \frac{\mathbf{n}}{r^2} \times Z\alpha f(r), \quad (8)$$

where Z is the atomic number, α is the fine structure constant and $f(r)$ is the fraction of nuclear charge within the radius r. For the uniform sphere charge distribution $f(r) = r^3/R_N^3$ for $r < R_N$ and $f(r) = 1$ for $r > R_N$. Substituting (8) and (6) into (4) and performing angular integration, we obtain intermediate expressions for d_N and S_N:

$$\frac{d_N}{eC_{E^3B}} = 4\pi(Z\alpha)^2 \int \frac{dr}{r^2} f^2\left(\frac{5}{3}b_1 + \frac{4}{3}b_2\right), \quad (9)$$

$$\frac{S_N}{eC_{E^3B}} = \frac{2\pi(Z\alpha)^2}{15}\int drf^2\left[b_1\left(11-\frac{25}{3}\frac{r_c^2}{r^2}\right)\right.$$
$$\left.+ b_2\left(16-\frac{20}{3}\frac{r_c^2}{r^2}\right)\right]. \qquad (10)$$

In these expressions, r_c^2 is the nuclear charge radius. We follow the standard definition of the Schiff moment that in nonrelativistic limit and pointlike nucleus leads to the effective nuclear-spin-dependent T, P-odd Hamiltonian for electrons

$$H_{T,P\text{-odd}} = -(S_N/e)\times 4\pi\alpha(\mathbf{n}_I\cdot\boldsymbol{\nabla}_e)\delta(\mathbf{r}_e). \qquad (11)$$

Nuclear dependence in (9) and (10) is encapsulated in f and b_i. Electric field, i.e., f, is determined by the collective properties of the nucleus and has little to no dependence on the details of the nucleon's wave function inside a large nucleus. In contrast, the scalar functions b_i that describe magnetization are determined by mostly "outside" valence nucleons and carry more detail about nuclear structure. For any realistic choice of f and b_i, however, it is easy to see that radial integrals will be saturated by distances $r\sim R_N$.

Specializing our calculations to the ^{199}Hg nucleus, we adopt a simple shell model description of it with a valence neutron in $n_r=2$, $l=1$, and $j=1/2$ state carrying all angular momentum dependence, and ignore configuration mixing. Its wave function can be conveniently written as

$$\psi(\mathbf{r}_n) = R_{2p}(r_n)\frac{(\boldsymbol{\sigma}_n\cdot\mathbf{n}_n)}{\sqrt{4\pi}}\chi, \qquad (12)$$

where $\mathbf{r}_n=\mathbf{n}_n r_n$ and χ are the neutron's coordinate and two component spinor, and R_{2p} is the radial wave function normalized as $\int R^2r^2dr=1$. Nuclear spin in this case coincides with j, and $\mathbf{n}_I=\chi^\dagger\boldsymbol{\sigma}_n\chi$. The magnetic moment of the nucleus has a simple connection to the magnetic moment of the neutron, $e\mu_N=(-1/3)e\mu_n=(-1/3)\times(-1.91)\times 4\pi\alpha/(2m_p)$. The magnetization functions b_i defined earlier in (6) can be directly related to radial R_{2p} functions, and explicit calculations give

$$b_1(r) = \frac{-1.91\alpha}{2m_p}\times\frac{2}{3}\left(2\int_r^\infty\frac{dr_n}{r_n}R_{2p}^2(r_n)-R_{2p}^2(r)\right),$$
$$b_2(r) = \frac{-1.91\alpha}{2m_p}\times\frac{1}{3}\left(R_{2p}^2(r)-\frac{1}{r^3}\int_0^r dr_n r_n^2R_{2p}^2(r_n)\right).$$

One can easily check that the corresponding boundary conditions (7) are satisfied. To learn about the parametric dependence of our answers we first explore the simplified case when not only the charge distribution but also $R(r)$ is taken to be constant inside the nuclear radius and zero outside, $R_{2p}^2(r)=3R_N^{-3}\theta(R_N-r)$ [7]. In this approximation we get

$$\frac{d_N}{eC_{E^3B}}=\frac{1.91\times 2\pi Z^2\alpha^3}{3m_pR_N^4};\quad \frac{S_N}{eC_{E^3B}}=\frac{1.91\times 39\pi Z^2\alpha^3}{245m_pR_N^2}, \qquad (13)$$

and consequently S_N scales as $Z^{4/3}$ since $R_N\propto Z^{1/3}$. In order to get a more realistic answer, we solve for R_{2p} numerically using the Woods-Saxon potential with parameters outlined in Ref. [32]. We check that our results reproduce $S_N(d_n)$ [7,32] with reasonable $\propto 30\%$ accuracy. Performing two numerical integrals over r_n and r, and substituting explicit expression for C_{E^3B}, we obtain the following numerical result,

$$S_{^{199}\mathrm{Hg}}/e \simeq (d_\mu/e)\times 4.9\times 10^{-7}\ \mathrm{fm}^2, \qquad (14)$$

that lands itself very close (within 20%) from the naive estimate (13). Given the experimental constraint of $|S_{^{199}\mathrm{Hg}}| < 3.1\times 10^{-13}\ e\,\mathrm{fm}^3$ [2], we arrive at the following final result

$$|d_\mu| < 6.4\times 10^{-20}\ e\,\mathrm{cm}, \qquad (15)$$

which is somewhat more stringent bound, by a factor of ~2.5 than (1). Result (14) carries a 25%–30% uncertainty due to neglected contributions from the nuclear orbital mixing.

Future developments may bring about new experiments that would search for EDMs involving nuclei with $I\geq 1$ [33], opening the possibility of measuring magnetic quadrupole moments, and using nuclei with large deformations and large Q_N. We perform a simple estimate for the expected size of the magnetic quadrupole by taking the electric field created by Q_N outside the nucleus, and cutting divergent integrals at R_N. This way, we arrive at the following estimate

$$\frac{M_N}{eC_{E^3B}}\sim\frac{48\pi Z^2\alpha^3}{5}\frac{Q_N}{e}\int\frac{dr}{r^5}\simeq\frac{Q_N}{e}\frac{12\pi Z^2\alpha^3}{5R_N^4}. \qquad (16)$$

Substituting expression (4), and normalizing electric quadrupole on large values observed in deformed nuclei, we get

$$\frac{M_N}{e}\sim 10^{-4}\ \mathrm{fm}\times\frac{Q_N}{e300\ \mathrm{fm}^2}\times(d_\mu/e). \qquad (17)$$

Taking typical matrix elements and extrapolating future sensitivity to the current one of the ThO experiment, one could probe $M_N/e\propto 10^{-11}\ \mathrm{fm}^2$ and consequently achieving $d_\mu/e\propto 10^{-20}\ e\,\mathrm{cm}$.

Muon EDM and paramagnetic CP-odd observables.— Finally we turn our attention to the electron-spin-dependent EDMs referred to as paramagnetic EDMs of atoms and molecules. These experiments probe the electron EDM operator [defined through Eq. (2) with $\mu\to e$] and semileptonic CP-odd operators among which the most important one is C_S,

$$\mathcal{L}_{eN} = C_S \frac{G_F}{\sqrt{2}} (\bar{e} i\gamma_5 e)(\bar{p}p + \bar{n}n). \tag{18}$$

For nonrelativistic electrons and a small R_N limit, this term gives rise to $\propto (\boldsymbol{\sigma}_e \cdot \boldsymbol{\nabla}_e)\delta(\mathbf{r}_e)$ effective interaction. The importance of C_S for probing CP violation in the Higgs sector, quark sector etc has been emphasized many times in the literature, see, e.g., [34–37]. Tremendous progress of the past decade with limits on d_e and C_S has been achieved by the ACME Collaboration in experiment with the ThO paramagnetic molecule [4]. Since the results are often reported in terms of d_e, it is convenient to introduce a linear combination of the two quantities limited in experiment and refer to them as "equivalent d_e" [38,39]:

$$d_e^{\text{equiv}} = d_e + C_S \times 1.5 \times 10^{-20}\ e\,\text{cm}. \tag{19}$$

Current experimental limit stands as $|d_e^{\text{equiv}}| < 1.1 \times 10^{-29}\ e\,\text{cm}$ [4].

Muon EDM contributes both to d_e and C_S through loops. The bona fide three-loop $d_e(d_\mu)$ computation, Fig. 2, was performed in [13],

$$d_e = d_\mu \left(\frac{\alpha}{\pi}\right)^3 \frac{m_e}{m_\mu} \times 1.92 \simeq 1.1 \times 10^{-10} d_\mu. \tag{20}$$

If the direct bound (1) is saturated, d_e will be larger than the experimental limit by about a factor of 2, as already noted in Ref. [21]. It turns out, however, that equivalent of C_S generated by E^3B interaction gives a larger contribution.

A representative diagram contributing to the T, P-odd electron-nucleus interaction via E^3B term is shown in Fig. 2. The two electric field lines can be sourced by a nucleon, or a nucleus, while the photon loop attached to the electron line generates a $m_e \bar{e} i\gamma_5 e$ interaction. There are two important considerations regarding this type of contribution: (i) The photon loop is enhanced by $\log(\Lambda/m_e)$, and we calculate this loop to logarithmic accuracy, cutting it at $\Lambda = m_\mu$. (In practice, this cutoff will be supplied by the nonlocal nature of the muon loop in Fig. 1.) (ii) In a large nucleus $\mathbf{E}^2$ is coherently enhanced and dominates over effects proportional to electromagnetic contribution of individual nucleons $\propto Z\langle p|\mathbf{E}^2|p\rangle$. Being concentrated inside and near the nucleus, $\mathbf{E}^2$ can be considered *equivalent* to the delta-functional contribution:

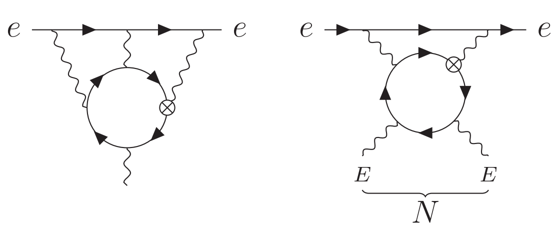

FIG. 2. Three-loop contribution to d_e and two-loop contribution to equivalent C_S generated by d_μ.

$$e^2(\mathbf{E}^2)_{\text{nucl}} \to \delta(\mathbf{r}) \times \frac{4\pi(Z\alpha)^2}{R_N} \times \int_0^\infty \frac{f^2(R_N x)}{x^2} dx, \tag{21}$$

where $x = r/R_N$. For a constant density charge distribution, the integral in (21) is 6/5, and we adopt this number. Putting the results of the loop calculation together with (21), and using the explicit form for C_{E^3B} we arrive at the following prediction for the *equivalent* C_S value:

$$\frac{G_F}{\sqrt{2}} C_S^{\text{equiv}} = \kappa \frac{4Z^2\alpha^4}{\pi A} \times \frac{m_e(d_\mu/e)}{m_\mu^3 R_N} \times \log\left(\frac{m_\mu}{m_e}\right). \tag{22}$$

As one can see, C_S^{equiv} scales as $Z^2 A^{-1} R_N^{-1} \propto Z^{2/3}$, which is the sign of coherent enhancement. A is the number of nucleons, and $A = 232$ for Th. In this expression, κ is a fudge factor to account for the change of the electronic matrix elements stemming from the fact that nuclear $\mathbf{E}^2$ extends beyond the nuclear boundary, while true nucleonic C_S effect is proportional to nuclear density and vanishes outside. Solving the Dirac equation near the nucleus for the outside $s_{1/2}$ and $p_{1/2}$ electron wave functions and finding a ratio of the matrix elements for these two distributions result in $\kappa \simeq 0.66$. We then arrive to the numerical result

$$C_S^{\text{equiv}} = 3.1 \times 10^{-10} \left(\frac{d_\mu}{10^{-20}\ e\,\text{cm}}\right). \tag{23}$$

Combining (23) with (20) into (19), we arrive at our main result

$$d_e^{\text{equiv}} \simeq 5.8 \times 10^{-10} d_\mu \Rightarrow |d_\mu| < 1.9 \times 10^{-20}\ e\,\text{cm}. \tag{24}$$

We observe that d_e and C_S^{equiv} interfere constructively, and C_S contribution is larger by a factor of $\simeq 4$. We believe (23) to be accurate within $\sim$15%–20% with uncertainties associated with modeling of $\mathbf{E}(r)$ and logarithmic approximation for the photon loop integral.

Outlook.—We have evaluated the electromagnetic transmission mechanisms of muon EDM to the observable EDMs that do not involve on-shell muons. We have found that muon-loop-induced E^3B effective interaction plays an important role and leads to novel indirect bounds, Eqs. (15) and (24) that are already stronger than the direct bound (1). Result (24) provides a new benchmark that future dedicated muon EDM experiments would have to overtake. We also notice that since both ^{199}Hg and ThO EDM results give an improvement, it is highly unlikely that a fine-tuned choice of d_e and hadronic CP violation would lead to the relaxation of indirect bounds on d_μ.

In this Letter, we do not discuss the short-distance physics that may lead to the enhanced d_μ. We note that while in some models d_μ is predicted at the same level as d_e, it is also feasible that d_μ/d_e scales as $(m_\mu/m_e)^3$ and possibly even larger. (Given the ongoing $g-2$ discrepancy in the muon sector, it is clear that d_μ deserves a separate treatment.) Still, it is instructive to equate d_μ to some simple scaling formula that involves an ultraviolet scale Λ_μ, and we choose $d_\mu = m_\mu/\Lambda_\mu^2$ scaling. Then our results translate to

$$\Lambda_\mu > 300 \text{ GeV}, \tag{25}$$

which underscores that the $(\text{weak scale})^{-1}$ distances start being probed. Depending on underlying model, there can be some scale dependence of the muon EDM form factor $d_\mu(Q^2)$ (see, e.g., [13]). This, however, does not obscure comparison of direct ($Q^2 \simeq 0$) and indirect ($Q^2 \simeq m_\mu^2$) limits derived in our Letter as long as the d_μ operator is generated at distances $\Lambda^{-1} \ll m_\mu^{-1}$.

We also update the limit on the τ-lepton EDM d_τ derived in [13]. Our analysis is directly applicable to d_τ after replacing m_μ by the τ-lepton mass m_τ. In this case, the electron EDM plays the dominant role since $d_e \propto m_\tau^{-1}$ while $S_N, C_S \propto m_\tau^{-3}$ up to logarithm. For the ThO molecule, we obtain

$$d_e^{\text{equiv}} \simeq 7.0 \times 10^{-12} d_\tau \Rightarrow |d_\tau| < 1.6 \times 10^{-18}\ e\,\text{cm}. \tag{26}$$

This surpasses the constraint from the Belle experiment [40]. The constraint from ^{199}Hg is weaker by a factor of $\sim 2 \times 10^2$ than (26).

Finally, while the focus of our Letter was on d_μ, one could also derive limits on C_{E^3B} applicable to other models. We get constraints on C_{E^3B} at the level of $10^{-41}\ \text{eV}^{-4}$ and better, which would be challenging to match with photon-based experiments [31].

This work was partly funded by the Deutsche Forschungsgemeinschaft under Germany's Excellence Strategy—EXC 2121 "Quantum Universe"—390833306. M. P. is supported in part by U.S. Department of Energy Grant No. desc0011842. The Feynman diagrams in this Letter are drawn with `TikZ-Feynman` [41].

*yohei.ema@desy.de
†gao00212@umn.edu
‡pospelov@umn.edu

[1] E. M. Purcell and N. F. Ramsey, Phys. Rev. **78**, 807 (1950).
[2] B. Graner, Y. Chen, E. G. Lindahl, and B. R. Heckel, Phys. Rev. Lett. **116**, 161601 (2016); **119**, 119901(E) (2017).
[3] W. B. Cairncross, D. N. Gresh, M. Grau, K. C. Cossel, T. S. Roussy, Y. Ni, Y. Zhou, J. Ye, and E. A. Cornell, Phys. Rev. Lett. **119**, 153001 (2017).
[4] V. Andreev *et al.* (ACME Collaboration), Nature (London) **562**, 355 (2018).
[5] C. Abel *et al.* (nEDM Collaboration), Phys. Rev. Lett. **124**, 081803 (2020).
[6] I. B. Khriplovich and S. K. Lamoreaux, *CP Violation Without Strangeness: Electric Dipole Moments of Particles, Atoms, and Molecules* (Springer, Singapore, 1997).
[7] J. S. M. Ginges and V. V. Flambaum, Phys. Rep. **397**, 63 (2004).
[8] M. Pospelov and A. Ritz, Ann. Phys. (Amsterdam) **318**, 119 (2005).
[9] J. Engel, M. J. Ramsey-Musolf, and U. van Kolck, Prog. Part. Nucl. Phys. **71**, 21 (2013).
[10] W. J. Marciano and A. Queijeiro, Phys. Rev. D **33**, 3449 (1986).
[11] S. Weinberg, Phys. Rev. Lett. **63**, 2333 (1989).
[12] S. M. Barr and A. Zee, Phys. Rev. Lett. **65**, 21 (1990); **65**, 2920(E) (1990).
[13] A. G. Grozin, I. B. Khriplovich, and A. S. Rudenko, Phys. At. Nucl. **72**, 1203 (2009).
[14] M. Davier, A. Hoecker, B. Malaescu, and Z. Zhang, Eur. Phys. J. C **77**, 827 (2017).
[15] G. Colangelo, M. Hoferichter, and P. Stoffer, J. High Energy Phys. 02 (2019) 006.
[16] M. Hoferichter, B.-L. Hoid, and B. Kubis, J. High Energy Phys. 08 (2019) 137.
[17] M. Davier, A. Hoecker, B. Malaescu, and Z. Zhang, Eur. Phys. J. C **80**, 241 (2020); **80**, 410(E) (2020).
[18] A. Keshavarzi, D. Nomura, and T. Teubner, Phys. Rev. D **101**, 014029 (2020).
[19] T. Aoyama *et al.*, Phys. Rep. **887**, 1 (2020).
[20] B. Abi *et al.* (Muon $g-2$ Collaboration), Phys. Rev. Lett. **126**, 141801 (2021).
[21] A. Crivellin, M. Hoferichter, and P. Schmidt-Wellenburg, Phys. Rev. D **98**, 113002 (2018).
[22] G. W. Bennett *et al.* (Muon $(g-2)$ Collaboration), Phys. Rev. D **80**, 052008 (2009).
[23] Y. K. Semertzidis *et al.*, AIP Conf. Proc. **564**, 263 (2001).
[24] H. Iinuma, H. Nakayama, K. Oide, K.-i. Sasaki, N. Saito, T. Mibe, and M. Abe, Nucl. Instrum. Methods Phys. Res., Sect. A **832**, 51 (2016).
[25] M. Abe *et al.*, Prog. Theor. Exp. Phys. **2019**, 053C02 (2019).
[26] A. Adelmann *et al.*, arXiv:2102.08838.
[27] L. I. Schiff, Phys. Rev. **132**, 2194 (1963).
[28] See Supplemental Material at http://link.aps.org/supplemental/10.1103/PhysRevLett.128.131803 for details of our calculations, which includes Ref. [29,30].
[29] L. D. Landau and E. M. Lifshits, *Quantum Mechanics: Non-Relativistic Theory*, Course of Theoretical Physics Vol. v.3 (Butterworth-Heinemann, Oxford, 1991), ISBN 978-0-7506-3539-4.
[30] V. B. Berestetskii, E. M. Lifshitz, and L. P. Pitaevskii, *Quantum Electrodynamics*, Course of Theoretical Physics Vol. 4 (Pergamon Press, Oxford, 1982), ISBN 978-0-7506-3371-0.
[31] M. Gorghetto, G. Perez, I. Savoray, and Y. Soreq, J. High Energy Phys. 10 (2021) 056.

[32] V. F. Dmitriev and R. A. Sen'kov, Phys. Rev. Lett. **91**, 212303 (2003).
[33] V. V. Flambaum, D. DeMille, and M. G. Kozlov, Phys. Rev. Lett. **113**, 103003 (2014).
[34] S. M. Barr, Phys. Rev. Lett. **68**, 1822 (1992).
[35] O. Lebedev and M. Pospelov, Phys. Rev. Lett. **89**, 101801 (2002).
[36] M. Jung and A. Pich, J. High Energy Phys. 04 (2014) 076.
[37] V. V. Flambaum, M. Pospelov, A. Ritz, and Y. V. Stadnik, Phys. Rev. D **102**, 035001 (2020).
[38] M. Pospelov and A. Ritz, Phys. Rev. D **89**, 056006 (2014).
[39] The sign convention of C_S can be checked, e.g., with V. A. Dzuba, V. V. Flambaum, and C. Harabati, Phys. Rev. A **84**, 052108 (2011). We define $\gamma_5 = i\gamma^0\gamma^1\gamma^2\gamma^3$ that has the opposite sign as theirs.
[40] K. Inami *et al.* (Belle Collaboration), Phys. Lett. B **551**, 16 (2003).
[41] J. Ellis, Comput. Phys. Commun. **210**, 103 (2017).